Polyoxometalates

DOI: 10.1002/anie.201402932

Time-Resolved Assembly of Cluster-in-Cluster $\{Ag_{12}\}$-in-$\{W_{76}\}$ Polyoxometalates under Supramolecular Control**

Caihong Zhan, Jamie M. Cameron, Jing Gao, Jamie W. Purcell, De-Liang Long, and Leroy Cronin**

Abstract: *We report the time-resolved supramolecular assembly of a series of nanoscale polyoxometalate clusters (from the same one-pot reaction) of the form: $[H_{(10+m)}Ag_{18}Cl(Te_3W_{38}O_{134})_2]_n$, where $n=1$ and $m=0$ for compound* ***1*** *(after 4 days), $n=2$ and $m=3$ for compound* ***2*** *(after 10 days), and $n=\infty$ and $m=5$ for compound* ***3*** *(after 14 days). The reaction is based upon the self-organization of two $\{Te_3W_{38}\}$ units around a single chloride template and the formation of a $\{Ag_{12}\}$ cluster, giving a $\{Ag_{12}\}$-in-$\{W_{76}\}$ cluster-in-cluster in compound* ***1****, which further aggregates to cluster compounds* ***2*** *and* ***3*** *by supramolecular Ag-POM interactions. The proposed mechanism for the formation of the clusters has been studied by ESI-MS. Further, control experiments demonstrate the crucial role that TeO_3^{2-}, Cl^-, and Ag^+ play in the self-assembly of compounds* ***1–3****.*

Polyoxometalates (POMs) are a class of discrete, polynuclear anionic metal oxo clusters that are commonly formed by the controlled self-assembly of early transition-metal oxo anions (primarily W, Mo, and V), often resulting in remarkably complex nanoscale architectures.[1] POMs occupy a unique 'mesoscopic' space between molecular oxo anions and infinite oxides, and offer unique possibilities for materials design at the nanoscale.[2–4] In polyoxotungstates, architectural control can be achieved at the fragment level by carefully selecting the heteroanion templates. In particular, we have been using anions such as $(SeO_3)^{2-}$ and $(TeO_3)^{2-}$, which can exert a powerful structure-directing effect as a result of the lone pair of the heteroanion,[5] itself templating massive structures.[6] In this way, it is possible to generate a diverse library of nucleophilic POM "secondary building units" (SBUs) which can serve as well-defined precursors in the formation of larger assemblies, which can be intricately controlled by the use of the heteroanion as well as linking coordinating cations.[7–11] However, discriminating the self-assembly, aggregation, and isolation of nanoscale POM species as a function of time, and while under supramolecular control, were especially difficult until now.

Herein, we report a new approach to polyoxometalate cluster assembly combining heteroanion, cation, and supramolecular encapsulation of chloride to control structural assembly and aggregation. This leads to the heteroatom-controlled assembly of a lacunary fragment, which is then organized around a supramolecular-chloride-templated $\{Ag_{12}Cl\}$ cluster, which itself is located within a $\{W_{76}\}$ superstructure, giving compound **1** ($\{Ag_{18}Cl(Te_3W_{38})_2\}$; see Figure 1). The supramolecular $\{Ag_{12}Cl\}$ cluster at the center

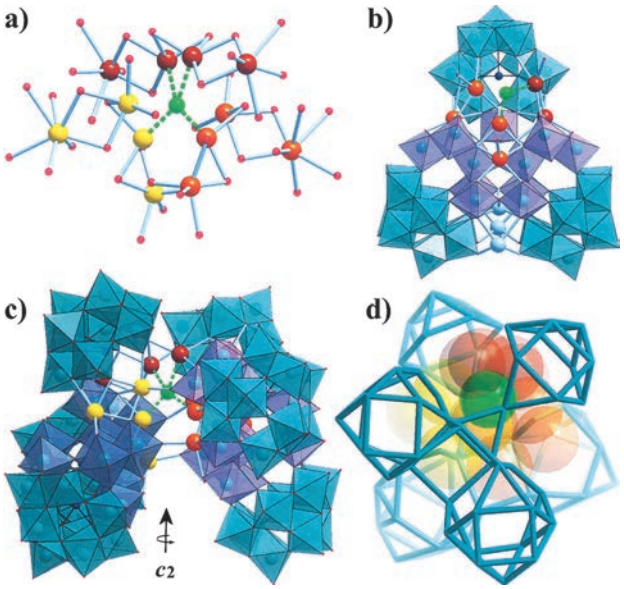

Figure 1. Structural aspects of **1**. a) $\{Ag_{12}Cl\}$ core with the four direct Ag–Cl bonding interactions shown. The three non-interacting groups of Ag cations are also highlighted. b) $\{Te_3W_{38}\}$ half unit found in **1–3** with the coordinated Ag^+ cations shown. c) The fully assembled structural unit of **1**. d) A pictographic representation of **1** highlighting the twisted orientation of the two $\{Te_3W_{38}\}$ half units with respect to another around the central $\{Ag_{12}Cl\}$ core. Cations and water molecules are omitted. ($\{TeW_9\}$ units are shown as teal/aqua polyhedra, $\{W_{11}\}$ units are shown in lavender/blue gray polyhedra. O: red, Te: dark blue, Ag: brown, orange, and gold, Cl: green).

of compound **1** is present in compounds **1–3**, all of which are comprised of the same repeating structural unit. These are linked into larger architectures by supramolecular Ag–cation interactions, meaning that both the building blocks and the assembly of the clusters are under supramolecular control. The key unit is the $\{Te_3W_{38}\}$ unit, which we hypothesize to be the essential component in the self-assembly and formation of compounds **1–3**.

[*] C. Zhan, J. M. Cameron, J. Gao, J. W. Purcell, D.-L. Long, L. Cronin
WestCHEM, School of Chemistry, The University of Glasgow
University Avenue, Glasgow G12 8QQ, Scotland (UK)
E-mail: deliang.long@glasgow.ac.uk
lee.cronin@glasgow.ac.uk
Homepage: http://www.croninlab.com

[**] We thank the EPSRC, WestCHEM and the University of Glasgow for supporting this work.

Supporting information for this article is available on the WWW under http://dx.doi.org/10.1002/anie.201402932.

We isolated three distinct compounds, which were formed sequentially as a function of time, by using a facile "one-pot" reaction from simple precursors. These three compounds are the giant 0D assemblies $(C_4H_{12}NO)_{22}Na_7[H_{10}Ag_{18}Cl(Te_3W_{38}O_{134})_2]\cdot 38H_2O$ (**1**) and $\{(C_4H_{12}NO)_{20}Na_6[H_{13}Ag_{18}Cl(Te_3W_{38}O_{134})_2]\cdot 35H_2O\}_2$ (**2**), and the 3D framework $\{(C_4H_{12}NO)_{18}Na_6[H_{15}Ag_{18}Cl(Te_3W_{38}O_{134})_2]\cdot 53H_2O\}_n$ (**3**). Compound **1** forms after 4 days, compound **2** after 10 days, and compound **3** after 14 days, and all of them have different crystal forms (see Scheme 1).

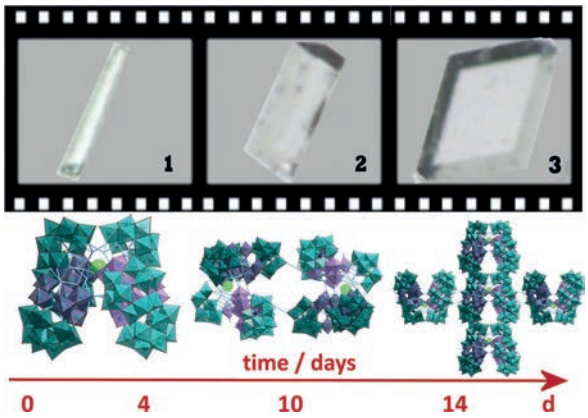

Scheme 1. Assembly pathway and time-resolved crystallization of compounds **1**–**3** from simple precursors to nanosized clusters and extended 3D frameworks. The ({TeW_9} units are shown in teal/aqua polyhedra, {W_{11}} units are shown in lavender/blue gray polyhedra. O: red, Te: dark blue, Cl: green. The {Ag_n} core and linkers are shown by the pale blue wireframe. The crystal shape, size, and content changes as a function of time in solution, giving **1** to **3** in sequence.

Compounds **1**–**3** were synthesized by the simple one-pot reaction of $Na_2WO_4\cdot 2H_2O$, Na_2TeO_3, 2-dimethylaminoethanol, and $AgNO_3$, and each of them could be reliably isolated from the same mother liquor by a time-resolved crystallization process. Notably, crystals of each species are first separated from the mother liquor before the subsequent species are grown. Each compound can be clearly identified by its unique crystal morphology and can be reliably isolated with good phase purity, purely as a function of time (Scheme 1). It is also important to note that both concentration and solubility effects on the crystallization of **1**–**3** do not appear to play a significant role (as the formation of **3**, which is the least soluble product, always occurs last and, significantly, is not reliant on the prior isolation of **1** and **2** from the mother liquor; the solubilities of compounds **1**, **2**, and **3** in $mg\,mL^{-1}$ are 2.28, 1.90, and 1.78, respectively). Similarly, the effect of the pH value on this system is expected to be minimal, owing to the buffering effect of 2-dimethylaminoethanol.

A detailed crystallographic analysis of **1** (the anion structure of which is also present in compounds **2** and **3**) reveals a complex molecular system based on a multi-layered assembly centered around a single Cl^- anion, which itself is encapsulated within the central {Ag_{12}} core located at the core of the cluster (Figure 1 c). Six Ag sites can be identified in the proximity of the Cl^- ion with Ag–Cl distances between 2.51 and 2.95 Å, four of which can be considered to have direct bonding interactions (with bond distances of 2.509–2.774 Å) in a distorted square-planar coordination environment (Figure 1 a). These silver(I) ions are further linked by μ_3- and μ_4-oxo bridges (shared with W centers on the supporting tungstate shell) into three distinct, non-interacting {Ag_4} units, which coordinate to the POM framework and are linked only through interactions with the encapsulated Cl^- (Figure 1 a). The POM framework that supports this {$Ag_{12}Cl$} is a well-defined superlacunary $[Te_3W_{38}O_{134}]^{28-}$ "half-unit", which itself can be viewed as a central, open-faced $[W_{11}O_{35}]^{4-}$ core supported by three tri-vacant $[TeW_9O_{33}]^{8-}$ clusters (Figure 1 b). The {W_{11}} moiety is unusual given its "open" structure, which is not analogous to similar compositions such as that reported by Lehmann et al.[12] Indeed, this open framework provides an excellent surface for the binding of Ag^+ ions, which can coordinate to both the exposed terminal oxo groups of the central {W_{11}} moiety and the available vacancies on the {TeW_9} lobes (Figure 1 b). In this way, the two {Te_3W_{38}} units assemble around the {$Ag_{12}Cl$} core in a face-to-face manner, with each "half-unit" off-set by about 65° (Figure 1 d), imposing chirality on the fully assembled {$Ag_{18}Cl(Te_3W_{38})_2$} anion, with a virtual C_2 symmetry and no mirror plane. The reduced symmetry of **1** therefore enables the existence of two enantiomeric forms of the aggregated structure, Λ and Δ, based on the organization of the {Te_3W_{38}} units (i.e., displaying either a left- or right-handed twist). Ultimately, **1** crystallizes as a purely racemic mixture in the centrosymmetric space group *P*-1.

Compounds **2** and **3** could be isolated from the same reaction mixture by crystallization after around 10 and 14 days, respectively. Compound **2**, which crystallizes in the same *P*-1 system as **1** and with a nearly identical unit cell, features one of the Λ and Δ enantiomers of the {$Ag_{18}Cl(Te_3W_{38})_2$} cluster linked by just two Ag–oxo bridges to give a single, giant, racemic POM structure with dimensions of 2.3 nm x 4.2 nm (Figure S1). In **3**, a racemic mixture of the Λ and Δ enantiomers are more extensively cross-linked into an extended 3D network, with tighter packing of the Ag-bridged {$Ag_{18}Cl(Te_3W_{38})_2$} units (Figure S2). The topology of **3** was also analyzed, showing that each {$Ag_{18}Cl(Te_3W_{38})_2$} cluster serves as a six-connected node by linking to six adjacent clusters (Figure S3), thus forming a six-connected network with a Schläfli symbol of $4^{11}\cdot 6^4$.[13]

To explore the role of the chloride template, we conducted synthetic studies in the absence of chloride, resulting in vastly reduced yields of the compounds (as a result of trace amounts of chloride present in glassware, reagents etc.). When chloride was added in the form of NaCl, the yields rose markedly, giving further evidence of the positive effect of chloride as a supramolecular template in the assembly of these giant structures. High-resolution negative-mode electrospray ionisation mass spectrometry (ESI-MS) was performed on single-crystalline samples to explore the stability of compounds **1**–**3** in solution (see the Supporting Information for more details). For all compounds, a series of sequentially charged peaks could be identified in the region of 1350–4000 *m*/*z* (Figure 2), where the major peaks in the spectra

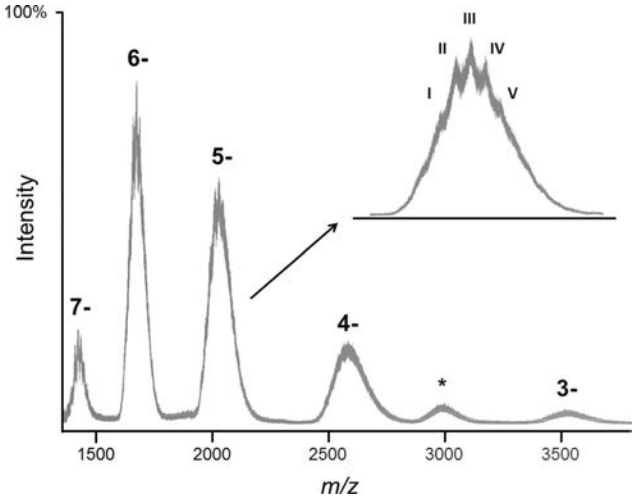

Figure 2. Negative-mode mass spectrum of **1** (also representative of spectra for **2** and **3**) in the *m*/*z* range of 1350–4000 showing the major peaks corresponding to sequentially charged fragments of the $\{Te_3W_{38}\}$ primary building unit. Inset: overlapping peaks comprising the "true" isotopic envelope for each major "peak" with those well-defined enough to be identified (highlighted I–V). Full spectral assignments are provided in the Supporting Information.

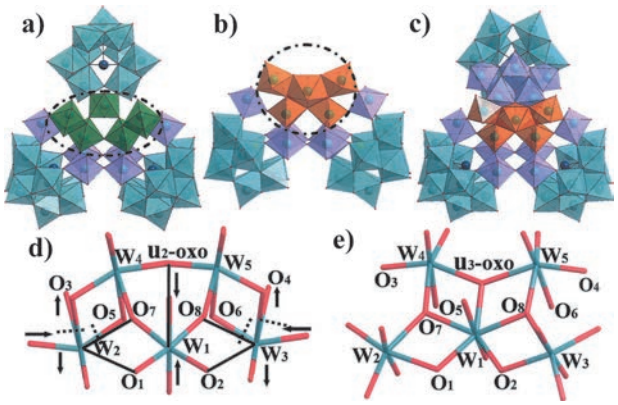

Figure 3. Comparison of two "cores" of the $\{Te_3W_{38}\}$ and $\{Te_3W_{43}\}$ species. a) Representation of the $\{Te_3W_{38}\}$ building block in compounds **1**–**3**. b) $\{Se_2W_{29}\}$ unit reported previously. c) $\{Te_3W_{43}\}$ building block in compound **4**. d) Open $\{W(W_2)_2\}$ core. e) Condensed $\{W(W_4)\}$ core. ($\{W(W_2)_2\}$ unit shown in green polyhedra and pentagonal unit $\{W(W_4)\}$ shown in orange. For comparison, the two "cores" are shown in wireframe mode (W: teal, O: red). The dashed line represents the breaking of a bond and the solid line the generation of a bond. Arrows show the direction of movement of atoms.

corresponded to the hypothesized $\{Te_3W_{38}\}$ intermediate unit. Additionally, multiple peaks corresponding to smaller $\{TeW_9\}$ units (which are the primary building blocks of the $\{Te_3W_{38}\}$ intermediate) could be identified in the lower *m*/*z* range of 750–1350 (see the Supporting Information). This is significant as it provides evidence for the viability of our hypothesized assembly pathway in the formation of **1**–**3** (see Scheme 1). Notably, the major peaks observed above 1350 *m*/*z* are very broad (with widths approximately 10 times larger than the simulated peaks) and, while this is not unusual for high-nuclearity POM species,[14] closer inspection clearly shows that this is due to the fact that each envelope is actually comprised of multiple overlapping peak envelopes (see Figure 2, inset).

These overlapping peaks correspond to $\{Te_3W_{38}\}$ fragments with different Ag^+ and Na^+ cations and can be assigned as: $[Ag_{a-x}Na_{b+x}H_{11}(Te_3W_{38}O_{134})]^{n-}$ (see Table S2). While none of the peaks in the spectra of **1**–**3** can be unambiguously assigned to the intact $\{Ag_{18}Cl(Te_3W_{38})_2\}$ unit, the peak located at around 2990 *m*/*z* (highlighted by the asterisk in Figure 2) may correspond to a related fragment, $[Na_{16}H_{22}\{Ag_{12}Cl(Te_3W_{38}O_{134})_2\}\cdot 10H_2O]^{7-}$ (calculated *m*/*z* = 2989.3). Unfortunately, despite our best efforts, we were unable to fully resolve the charge of this peak, hence this assignment can only be made tentatively at this time.

The mass spectrometry data also suggest the important role the Ag^+ cations play in effectively trapping the unusual $\{W_{11}\}$ moiety on the $\{Te_3W_{38}\}$ building unit. The remarkably open, or uncondensed, structure of the $\{W_{11}\}$ framework, which has an especially high number of external (i.e. non-bridging) oxo groups, would otherwise most likely be unstable without extensive chelation to the highly coordinatively flexible Ag^+ ions. A simple control experiment confirms this hypothesis, as a new species $Na_7K_{10}(C_4H_{12}NO)_7[H_2Te_3W_{43}O_{148}]\cdot 42H_2O$ (**4**) (Figure 3c), which is structurally very similar to the $\{Te_3W_{38}\}$ species (Figure 3a), is the only product formed when Ag^+ is absent from the reaction system and K + cations are present as the counterion. Furthermore, the importance of the structure-directing Te^{IV} heteroatoms can be demonstrated in the same way, producing a far simpler silver-linked network when the TeO_3^{2-} is similarly absent, giving $(C_4H_{12}NO)Na_7[HAg_3W_{12}O_{42}]\cdot 25H_2O$ (**5**) (Figure S4). This compound is based around the condensed $\{W_{12}\}$ isopolytungstate unit (see the Supporting Information for more detail on the structural characterization of **5**).

Crystallographic analysis of **4** confirms that the structure is closely related to that of the $\{Te_3W_{38}\}$ building unit observed in **1**–**3**. It also contains three $\{TeW_9\}$ units arranged around a central $\{W_{16}\}$ tungstate core, which contains an interesting monolacunary $\{W(W_4)\}$ pentagonal unit that has recently been reported by our group.[15] Indeed, an alternative interpretation of the structure of **4** is that it is simply an extended analogue of the previously reported $\{Se_2W_{29}\}$ cluster (Figure 3b), in which the "base" of **4** is an analogous $\{Te_2W_{29}\}$ unit that has further condensed with an additional $\{W_3\}$ unit, itself linked in turn by two $\{W_1\}$ linkers to a third $\{TeW_9\}$ cluster. Furthermore, this compound represents the first example of the pentagonal unit $\{W(W_4)\}$ discovered in a Te-containing polyoxotungstate. ESI-MS was also used to characterize **4**, more details can be found in the Supporting Information.

In summary, we have shown how a simple one-pot strategy that employs structure-directing TeO_3^{2-} heteroions and electrophilic Ag^+ linkers can give rise to a remarkable series of structurally complex, high-nuclearity polyoxotungstates, which can be isolated by a process of time-resolved crystallization. These clusters range from a discrete, 0D species through to an extended 3D network based on a repeating, Ag-supported $\{Te_3W_{38}\}$ intermediate building block, two of which form chiral aggregates. Notably, **2** is by far

the highest-nuclearity, discrete, noble-metal-containing POM reported to date. This proposed mechanism for the formation of **1**–**3** has been confirmed by ESI-MS studies, and the vital, supramolecular templating effect of the encapsulated Cl^- ion has been empirically confirmed. Furthermore, two new POM species have been discovered by exploring the crucial role that both TeO_3^{2-} and Ag^+ play in the self-assembly of **1**–**3**, one of which (**4**) contains a rare example of a pentagonal {W(W$_4$)} unit. This work serves to illustrate the vast potential of using soft cations like silver in the assembly of gigantic molecular metal oxide nanostructures.

Experimental Section

Synthesis of $(C_4H_{12}NO)_{22}Na_7[H_{10}Ag_{18}Cl(Te_3W_{38}O_{134})_2]\cdot 38H_2O$ **1**: $Na_2WO_4\cdot 2H_2O$ (4.8 g, 14.5 mmol), Na_2TeO_3 (0.28 g, 1.3 mmol), and 2-dimethylaminoethanol (≥ 99.5 %, 2.4 mL) were dissolved in H_2O (50 mL). The pH value was adjusted to 4–4.5 by addition of nitric acid (75 %). $AgNO_3$ (0.26 g, 1.5 mmol) was added to the solution, which was then stirred for about 3 min. Finally, a small amount of NaCl (ca. 0.1 mg) was added to the solution, which was filtered and left for evaporation. Colourless needle-shaped crystals were obtained within four days. Yield: 0.032 g, (0.7 %, based on tungsten). IR: 3333 (w), 3058 (w), 2741 (w), 1072(w), 1624.9 (m), 1466.1 (m), 963.5 (s), 787.3 (s), 661.4 (s). Elemental analysis, calcd for $C_{88}H_{350}$ $Cl_1N_{22}O_{328}$ $Na_7Ag_{18}Te_6W_{76}$: C 4.43, H 1.48, N1.29, Na 0.68, Te 3.21, Ag 8.14, W 58.6 %; found C 4.21, H 1.21, N 1.25, Na 0.6, Te 3.38, Ag 7.95, W 58.1 %. TGA water loss from 20 to 95 °C, calcd (found) %: 2.8 (2.75).

Synthesis of $(C_4H_{12}NO)_{20}Na_6[H_{13}Ag_{18}Cl(Te_3W_{38}O_{134})_2]\cdot 35H_2O$ **2**: Compound **2** may be isolated from the same mother liquor as **1**. Once crystals of **1** had been isolated, the remaining solution was allowed to continue to slowly evaporate at room temperature. Colorless bar-shaped crystals were obtained within ten days. Yield: 0.022 g, (0.5 %, based on tungsten). IR: 3342 (w), 3058 (w), 2741 (w), 1068(w), 1623 (m), 1464(m), 952.9 (s), 784 (s), 663 (s). Elemental analysis, calcd for $C_{80}H_{323}Cl_1N_{20}O_{323}Na_6Ag_{18}Te_6W_{76}$: C 4.07, H 1.38, N 1.19, Na 0.58, Te 3.25, Ag 8.23, W 59.24 %; found C 3.98, H 1.12, N 1.25, Na 0.59, Te 3.60, Ag 7.81, W 58.91 %. TGA water loss from 20 to 109 °C, calcd (found) %: 2.7 (2.68).

Synthesis of $(C_4H_{12}NO)_{18}Na_6[H_{15}Ag_{18}Cl(Te_3W_{38}O_{134})_2]\cdot 53H_2O$ **3**: Compound **3** may be isolated from the same mother liquor as **1** and **2**. Once crystals of **1** and **2** had been isolated, the remaining solution was allowed to continue to slowly evaporate at room temperature. Colorless block-shaped crystals were obtained within two weeks. Yield: 0.36 g, (7.8 %, based on tungsten). IR: 3328 (w), 3062 (w), 2741 (w), 1068(w), 1618 (m), 1464(m), 952 (s), 858 (s), 788 (s), 667 (s). Elemental analysis, calcd for $C_{72}H_{337}$ $Cl_1N_{18}O_{339}$ $Na_6Ag_{18}Te_6W_{76}$: C 3.64, H 1.43, N 1.06, Na 0.58, Te 3.23, Ag 8.18, W 58.87 %; found C 3.7, H 1.38, N 1.08, Na 0.58, Te 3.20, Ag 8.18, W 58.7 %. TGA water loss from 20 to 96 °C, calcd (found) %: 4.0 (4.7).

Synthesis of $(C_4H_{12}NO)_7Na_7K_{10}[H_2Te_3W_{43}O_{148}]\cdot 42H_2O$ **4**: $Na_2WO_4\cdot 2H_2O$ (4.8 g, 14.5 mmol), Na_2TeO_3 (0.28 g, 1.3 mmol), and 2-dimethylaminoethanol (≥ 99.5 %, 2.4 mL) were dissolved in H_2O (50 mL). The pH value of the mixture was adjusted to 4–4.5 by addition of nitric acid (75 %) and the mixture was stirred for about 3 min. Finally, KCl (0.38 g, 5.1 mmol) was added to the solution, which was then filtered and left for evaporation. Colourless block-shaped crystals were obtained within one week. Yield: 1.24 g, (28.7 %, based on tungsten). IR: 1072(w), 3375 (m), 1627(m), 1464(m), 960.8 (m), 863 (m), 779(s), 695(s), 620.5 (s). Elemental analysis, calcd for $C_{28}H_{170}N_7O_{197}K_{10}Na_7Te_3W_{43}$: C 2.67, H 1.36, N 0.78, Na 1.28, K 3.1, W 62.75 %; found C 2.78, H 1.4, N 0.91, Na 1.23, K 2.8, W 63.6 %. TGA water loss from 20 to 140 °C, calcd (found) %: 5.8 (6.0).

Synthesis of $(C_4H_{12}NO)Na_7[HAg_3W_{12}O_{42}]\cdot 25H_2O$ **5**: $Na_2WO_4\cdot 2H_2O$ (4.8 g, 14.5 mmol) and 2-dimethylaminoethanol (≥ 99.5 %, 2.4 mL) were dissolved in H_2O (50 mL). The pH value of the mixture was adjusted to 4–4.5 by addition of nitric acid (75 %) and the mixture was stirred for about 3 min. After the addition of $AgNO_3$ (0.26 g, 1.5 mmol), the solution was stirred for about 3 min, then filtered and left for evaporation. Colorless block-shaped crystals were obtained within two weeks. Yield: 0.92 g, (19.2 %, based on tungsten). IR: 2112.2 (w), 933(m), 863 (m), 3347.1 (s), 1627.3 (s), 681.5 (s). Elemental analysis, calcd for $C_4H_{63}NO_{68}Na_7Ag_3W_{12}$: C 1.23, H 1.63, N 0.36, Na 4.12, Ag 8.29, W 56.51 %; found C 1.34, H 1.41, N 0.28, Na 4.27, Ag 8.13, W 57.1 %. TGA water loss from 20 to 200 °C, calcd (found) %: 11.5 (11.8).

Note: several organic amines have been employed in the course of exploring this reaction system, including 2-dimethylamino-1-propanol, triethylamine, trimethylamine, N-ethyldiisopropyl amine, and N-methyl diethanol amine. However, diffraction-quality crystals of compounds **1**–**3** only formed in the presence of 2-dimethylaminoethanol.

Detailed X-ray data for compounds **1**–**5** can be found in the Supporting Information. X-ray diffraction intensity data were measured at 150(2) K on an Oxford Diffraction Gemini A Ultra or Bruker Apex II Quasar diffractometers using $Mo_{K\alpha}$ [$\lambda = 0.71073$ Å]. Structure solution and refinement were carried out with SHELXS-97 and SHELXL-97 via WinGX. Corrections for incident and diffracted beam absorption effects were applied using analytical methods. CCDC 988045, 988046, 988047, 988048, and 988049 contain the supplementary crystallographic data for this paper. These data can be obtained free of charge from The Cambridge Crystallographic Data Centre via www.ccdc.cam.ac.uk/data_request/cif.

Received: March 2, 2014
Published online: August 1, 2014

Keywords: cluster compounds · nanostructures · self-assembly · supramolecular chemistry · polyoxometalates

[1] a) A. Dolbecq, E. Dumas, C. R. Mayer, P. Mialane, *Chem. Rev.* **2010**, *110*, 6009 – 6048; b) T. Liu, E. Diemann, H. Li, A. W. M. Dress, A. Müller, *Nature* **2003**, *426*, 59 – 62; c) D.-L. Long, R. Tsunashima, L. Cronin, *Angew. Chem.* **2010**, *122*, 1780 – 1803; *Angew. Chem. Int. Ed.* **2010**, *49*, 1736 – 1758; d) A. Müller, P. Gouzerh, *Chem. Soc. Rev.* **2012**, *41*, 7431 – 7463.

[2] a) A. Proust, B. Matt, R. Villanneau, G. Guillemot, P. Gouzerh, G. Izzet, *Chem. Soc. Rev.* **2012**, *41*, 7605 – 7622; b) Y.-F. Song, R. Tsunashima, *Chem. Soc. Rev.* **2012**, *41*, 7384 – 7402; c) H.-Y. Zang, H. N. Miras, D.-L. Long, B. Rausch, L. Cronin, *Angew. Chem.* **2013**, *125*, 7041 – 7044; *Angew. Chem. Int. Ed.* **2013**, *52*, 6903 – 6906; d) F. Xu, H. N. Miras, R. A. Scullion, D.-L. Long, J. Thiel, L. Cronin, *Proc. Natl. Acad. Sci. USA* **2012**, *109*, 11609 – 11612.

[3] a) Y. Ren, Z. Ma, P. G. Bruce, *Chem. Soc. Rev.* **2012**, *41*, 4909 – 4927; b) S. A. Barnett, N. R. Champness, *Coord. Chem. Rev.* **2003**, *246*, 145 – 168; c) A. R. Pease, J. O. Jeppesen, J. F. Stoddart, Y. Luo, C. P. Collier, J. R. Heath, *Acc. Chem. Res.* **2001**, *34*, 433 – 444.

[4] a) X. Fang, L. Hansen, F. Haso, P. Yin, A. Pandey, L. Engelhardt, I. Slowing, T. Li, T. Liu, M. Luban, D. C. Johnston, *Angew. Chem.* **2013**, *125*, 10694 – 10698; *Angew. Chem. Int. Ed.* **2013**, *52*, 10500 – 10504; b) H. Gleiter, *Acta Mater.* **2000**, *48*, 1 – 29; c) D.-L. Long, E. Burkholder, L. Cronin, *Chem. Soc. Rev.* **2007**, *36*, 105 – 121.

[5] a) J. Yan, D.-L. Long, L. Cronin, *Angew. Chem.* **2010**, *122*, 4211 – 4214; *Angew. Chem. Int. Ed.* **2010**, *49*, 4117 – 4120; b) J. Gao, J. Yan, S. Beeg, D.-L. Long, L. Cronin, *Angew. Chem.* **2012**, *124*, 3429 – 3432; *Angew. Chem. Int. Ed.* **2012**, *51*, 3373 – 3376.

[6] a) R. S. Winter, J. Yan, C. Busche, J. S. Mathieson, A. Prescimone, E. K. Brechin, D.-L. Long, L. Cronin, *Chem. Eur. J.* **2013**,

19, 2976 – 2981; b) J. M. Cameron, J. Gao, D.-L. Long, L. Cronin, *Inorg. Chem. Frontiers* **2014**, *1*, 178 – 185; c) J. Yan, D.-L. Long, E. F. Wilson, L. Cronin, *Angew. Chem.* **2009**, *121*, 4440 – 4444; *Angew. Chem. Int. Ed.* **2009**, *48*, 4376 – 4380; d) J. M. Cameron, J. Gao, L. Vilà-Nadal, D.-L. Long, L. Cronin, *Chem. Commun.* **2014**, *50*, 2155 – 2157.

[7] a) W.-C. Chen, H.-L. Li, X.-L. Wang, K.-Z. Shao, Z.-M. Su, E.-B. Wang, *Chem. Eur. J.* **2013**, *19*, 11007 – 11015; b) A. C. Stowe, S. Nellutla, N. S. Dalal, U. Kortz, *Eur. J. Inorg. Chem.* **2004**, 3792 – 3797.

[8] a) O. Oms, A. Dolbecq, P. Mialane, *Chem. Soc. Rev.* **2012**, *41*, 7497 – 7536.

[9] a) O. Fuhr, S. Dehnen, D. Fenske, *Chem. Soc. Rev.* **2013**, *42*, 1871 – 1906; b) Y. Kikukawa, Y. Kuroda, K. Yamaguchi, N. Mizuno, *Angew. Chem.* **2012**, *124*, 2484 – 2487; *Angew. Chem. Int. Ed.* **2012**, *51*, 2434 – 2437; c) H. I. S. Nogueira, F. A. A. Paz, P. A. F. Teixeira, J. Klinowski, *Chem. Commun.* **2006**, *0*, 2953 – 2955.

[10] a) C. E. Anson, A. Eichhöfer, I. Issac, D. Fenske, O. Fuhr, P. Sevillano, C. Persau, D. Stalke, J. Zhang, *Angew. Chem.* **2008**, *120*, 1346 – 1351; *Angew. Chem. Int. Ed.* **2008**, *47*, 1326 – 1331; b) C. Streb, R. Tsunashima, D. A. MacLaren, T. McGlone, T. Akutagawa, T. Nakamura, A. Scandurra, B. Pignataro, N. Gadegaard, L. Cronin, *Angew. Chem.* **2009**, *121*, 6612 – 6615; *Angew. Chem. Int. Ed.* **2009**, *48*, 6490 – 6493; c) X. Wang, N. Li, A. Tian, J. Ying, G. Liu, H. Lin, J. Zhang, Y. Yang, *Dalton trans.* **2013**, *42*, 14856 – 14865; d) Y.-P. Xie, T. C. W. Mak, *J. Am. Chem. Soc.* **2011**, *133*, 3760 – 3763.

[11] a) T. McGlone, C. Streb, D.-L. Long, L. Cronin, *Adv. Mater.* **2010**, *22*, 4275 – 4279; b) N. V. Izarova, M. T. Pope, U. Kortz, *Angew. Chem.* **2012**, *124*, 9630 – 9649; *Angew. Chem. Int. Ed.* **2012**, *51*, 9492 – 9510.

[12] T. Lehmann, J. Z. Fuchs, *Z. Naturforsch. B* **1988**, *43*, 89.

[13] O. V. Dolomanov, A. J. Blake, N. R. Champness, M. Schroder, *J. Appl. Crystallogr.* **2003**, *36*, 1283 – 1284.

[14] This phenomenon, which is common particularly in high-nuclearity POM clusters as a result of the exchange of cations or associated solvent, makes the assignment of peaks difficult. However, the relationship of the major peaks in each spectrum allows us to unambiguously identify them as sequentially charged anions containing the cluster of interest, particularly where the peak envelope is poorly resolved or especially broadened. Compounds **1**–**3** are unusual in that the overlapping peaks can be clearly delineated for those envelopes with the highest intensities as a result of the exchange of heavy Ag^+ cations, which offers greater separation between each individual species in the main envelope.

[15] J. Gao, J. Yan, S. Beeg, D.-L. Long, L. Cronin, *J. Am. Chem. Soc.* **2013**, *135*, 1796 – 1805.

